JOURNAL OF IRON AND STEEL RESEARCH, INTERNATIONAL. 2012, 19(1): 23-30

Looper-Tension Sliding Mode Control for Hot Strip Finishing Mills

ZHONG Zhao-zhun[1], WANG Jing-cheng[1], ZHANG Jian-min[2], LI Jia-bo[2]

(1. Department of Automation, Key Laboratory of System Control and Information Processing of Ministry of Education, Shanghai Jiaotong University, Shanghai 200240, China; 2. Baosteel Research Institute, Baoshan Iron and Steel Co Ltd, Shanghai 201900, China)

Abstract: An innovative sliding mode controller for looper and tension control in hot strip finishing mills was developed based on approximately linearized model. Firstly, a fictitious controller of the reduced order subsystem was designed according to desired dynamics, by which, the angle and tension loops were decoupled on the sliding manifold. Then, a sliding mode controller was used to validate finite time convergence of the state vector to the manifold which guaranteed the stability and performances of the overall system. This solution was considered owing to its well-known robustness and simplicity characteristics concerning disturbances and unmodelled dynamics. Simulation results showed the effectiveness of the proposed controller compared with conventional ones.

Key words: sliding mode control; looper control; tension control; hot strip finishing mill

Symbol List

d——Strip width;
g——Gravitational constant;
h——Strip exit thickness;
H——Strip entry thickness;
K——Steel deformation resistance;
$L'(\theta)$——Geometric looper length between stands;
$l_1(\theta)$——Distance between stand i and looper roll;
$l_2(\theta)$——Distance between looper roll and stand $i+1$;
L——Distance between two stands;
L_1——Distance between stand i and looper pivot;
L_2——Distance between looper pivot and stand $i+1$;
L_3——Distance between actual pass line and looper pivot;
L_G——Distance between pivoting point and gravity center of looper;
L_L——Looper arm length;
M_L——Looper mass;
R_r——Radius of looper roll;
R_w^i——Work roll radius of stand i;
R_w^{i+1}——Work roll radius of stand $i+1$;
S——Laplace variable;
S_b^{i+1}——Backward slip;
S_f^i——Forward slip;
t——Time variable;
$v_R^i(t)$——Work roll speed of stand i;
$v_R^{i+1}(t)$——Work roll speed of stand $i+1$;
$v_{sl}^i(t)$——Strip speed leaving upstream stand i;
$v_{se}^{i+1}(t)$——Strip speed entering downstream stand $i+1$;
α——Upstream strip angle;
β——Downstream strip angle;
θ——Looper angle;
$\xi(t)$——Deviation of interstand strip length with respect to L;
ρ——Steel density;
σ——Strip tension;
ω——Looper angular speed.

In the iron and steel industry, the role of hot strip mill is to roll the slabs into strips. During the casting process, a continuous steel slab is made and cut into bars. The bars, whose thicknesses are about 250 mm, are reheated up to a temperature around 1240 ℃ in a furnace and then rolled on the reversing roughing mills by making several passes. At the end of this roughing process, the steel strips are typically 30—35 mm in thickness and their temperatures are about 1050 ℃. After the roughing process, the strips pass through the crop shear before entering six or seven close coupled finishing mills. The objective of

Foundation Item: Item Sponsored by National Natural Science Foundation of China (60934007, 61174059); Program for New Century Excellent Talents of China (NCET-08-0359); Shanghai Rising-Star Tracking Program of China (11QH1401300)

Biography: ZHONG Zhao-zhun(1980—), Male, Doctor; **E-mail**: ZhaozhunZhong@hotmail.com; **Received Date**: November 24, 2010

hot strip finishing mill is to make further reduction of thickness and produce strips with thickness of 0.8—20 mm which are cooled down on run-out tables and finally coiled at the down coiler. The dimensional quality is controlled mainly by dedicated control systems such as AGC (automatic gauge control)[1], AWC (automatic width control)[2] and ASC (automatic shape control)[3].

Besides, stable mill operation through smooth threading of the strip is achieved by mass flow control, which is used to balance the input and output flow of a strip in a stand. Each rolling stand is driven by a main motor which controls speed from ASR (automatic speed regulator). It was experienced that during strip threading, strip tension is critical to strip quality and stable operation of the process[4]. Therefore, between each pair of rolling stands, it is equipped with a looper system, which is used to maintain upward pressure on the strip and keep the strip tension at a desired value during operation. The looper arm movement provides variation in strip storage length between the two stands to relax the mass flow unbalance and fluctuations. Thus, the looper angle should be kept at a desired constant value for giving the system some leeway to absorb abnormal large changes in looper length. Furthermore, looper and tension control is the key to the strip quality and successful mill operations. There are several factors, such as significant parameter uncertainties, disturbances and nonlinear nature of the system, making looper and tension control design challenge. For the last three decades, several control schemes, such as conventional PID (proportional integral derivative), decoupling[5-7], H-infinity[8], ILQ (inverse linear quadratic), and so on, have been proposed in the looper and tension control system. Recently, SMC (sliding mode control), which is well-known for its robustness, is adopted in Ref. [9] to design an innovative friction compensation controller. And in Ref. [10] the usage of integral variable structure control in the hydraulic looper system is also considered. However, in Ref. [9], the authors replaced the conventional PI controller with the SMC technique in the angle loop while the tension loop remains the conventional one. And as a common drawback of the fully nonlinear approach, the nonlinear controller proposed therein is rather complicated and might not be quite suitable for application on PLC (programmable logic controller) based plants. In this paper, a SMC controller is developed, which is simple in architecture and more adequate for application in both angle and tension loops based on the approximately linearized model of the system. And the angle and tension loops are decoupled in the stage of reduced order subsystem design. Once the sliding mode starts, the system is decoupled despite disturbances and unmodelled dynamics, which will improve the accuracy and performances of the overall system.

1 Process Model

The looper and tension model description follows closely that in Ref. [9] and forms the background of the control problem. The looper and interstand geometry is given in Fig. 1.

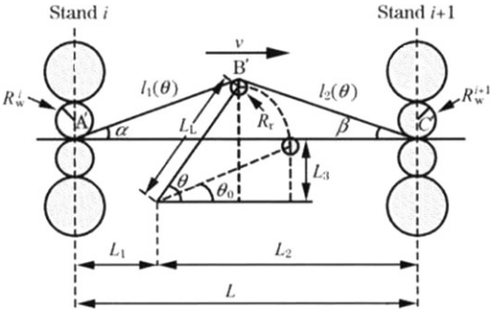

Fig. 1 Looper and interstand geometry

1.1 Tension dynamics

Strip tension at interstand is defined by the strip stretch and Young's modulus E of the strip:

$$\sigma(t)=E\left\{\frac{L'(\theta)-[L+\xi(t)]}{L+\xi(t)}\right\} \quad \text{for} \quad L'(\theta)>[L+\xi(t)] \tag{1}$$

where, $L+\xi(t)$ is the accumulated material length which changes due to the mass flow difference of the strip between stands. $L'(\theta)$ is evaluated as follows (Fig. 1):

$$L'(\theta)=l_1(\theta)+l_2(\theta) \tag{2}$$

$$l_1(\theta)=\sqrt{(L_1+L_L\cos\theta)^2+(L_L\sin\theta+R_r-L_3)^2} \tag{3}$$

$$l_2(\theta)=\sqrt{(L_2-L_L\cos\theta)^2+(L_L\sin\theta+R_r-L_3)^2} \tag{4}$$

and $\xi(t)$ is evaluated as follows:

$$\dot{\xi}(t)=v_{sl}^i(t)-v_{se}^{i+1}(t)+w_\xi(t) \tag{5}$$

and

$$v_{sl}^i(t)-v_{se}^{i+1}(t)=(1+S_f^i)v_R^i(t)-(1-S_b^{i+1})v_R^{i+1}(t) \tag{6}$$

where, $v_{sl}^i(t)$ depends on $v_R^i(t)$ and S_f^i which occurs between the work rolls and the strip; $v_{se}^{i+1}(t)$ depends on $v_R^{i+1}(t)$ and S_b^{i+1}; $w_\xi(t)$ represents unmodelled perturbations; S_f^i and S_b^{i+1} are sensitive to the tension σ and are evaluated as follows:

$$S_f^i=\frac{R_w^i}{h_i}\gamma_i^2 \tag{7}$$

and

$$S_b^{i+1}=1-\frac{h_{i+1}}{h_i}(1+S_f^{i+1}) \tag{8}$$

where

$$\gamma_i=\sqrt{\frac{h_i}{R_w^i}}\tan\left[\frac{1}{2}\arctan\sqrt{\frac{\varepsilon_i}{1-\varepsilon_i}}+\frac{\pi}{8}\ln(1-\varepsilon_i)\sqrt{\frac{h_i}{R_w^i}}+\frac{1}{2}\sqrt{\frac{h_i}{R_w^i}}\left(\frac{\sigma_i}{K}-\frac{\sigma_{i-1}}{K}\right)\right] \tag{9}$$

$$\varepsilon_i=\frac{h_{i-1}-h_i}{h_{i-1}} \tag{10}$$

σ_i represents the strip tension between stand i and stand $i+1$ while σ_{i-1} is the strip tension between stand $i-1$ and stand i; h_{i-1}, h_i and h_{i+1} represent strip exit thickness of stand $i-1$, i and $i+1$, respectively.

As far as the ith looper is concerned, for the sake of simplicity, $\sigma_i=\sigma$, $h_i=h$ and it is assumed that σ_{i-1}, σ_{i+1}, $v_R^{i+1}(t)$ are invariant.

It is necessary to point out that $\xi(t)$ in Eqn. (1) is rather small compared with L. As a result, $L+\xi(t)$ can be approximated by L. However, $\xi(t)$ can not be ignored in the numerator of Eqn. (1) because $L'(\theta)-L$ and $\xi(t)$ are of the same order of magnitude. Thus, the derivative of $\sigma(t)$ is

$$\dot\sigma(t)=\frac{E}{L}\left[\frac{\mathrm{d}}{\mathrm{d}t}L'(\theta)-\dot\xi(t)\right]=\frac{E}{L}\{L_L[\sin(\theta+\beta)-\sin(\theta-\alpha)]\dot\theta(t)-[(1+S_f^i)v_R^i(t)-(1-S_b^{i+1})v_R^{i+1}+w_\xi(t)]\} \tag{11}$$

where

$$\alpha=\tan^{-1}[(L_L\sin\theta-L_3+R_r)/(L_1+L_L\cos\theta)] \tag{12}$$

$$\beta=\tan^{-1}[(L_L\sin\theta-L_3+R_r)/(L_2-L_L\cos\theta)] \tag{13}$$

1.2 Looper dynamics

Apply Newton's law of motion to the looper system, the following equation can be obtained:

$$J\ddot\theta(t)=T_u(t)-T_{load}(\theta)+w_\omega(t) \tag{14}$$

where, J is the total inertia of the looper with respect to the pivoting point; $T_u(t)$ denotes the actuator torque on the looper; $T_{load}(\theta)$ represents the load torque on the looper; and $w_\omega(t)$ denotes the unmodelled dynamics. $T_{load}(\theta)$ is the combination of the loads caused by strip tension $T_\sigma(\theta)$, strip gravity $T_s(\theta)$ and looper gravity $T_L(\theta)$:

$$T_{load}(\theta)=T_\sigma(\theta)+T_s(\theta)+T_L(\theta) \tag{15}$$

where

$$T_\sigma(\theta)=\sigma hdL_L[\sin(\theta+\beta)-\sin(\theta-\alpha)] \tag{16}$$

$$T_L(\theta)=gM_LL_G\cos\theta \tag{17}$$

$$T_s(\theta)\approx 0.5g\rho Lhd L_L\cos\theta \tag{18}$$

1.3 Approximately linearized state space model

As for the actuators, $v_R^i(t)$ is controlled by ASR and $T_u(t)$ is controlled by ATR (automatic torque regulator), which are both modelled as first-order systems. From Eqn. (11) and Eqn. (14), the overall system can be described by the following nonlinear state model:

$$\begin{aligned}
\dot\theta(t)&=\omega(t)\\
\dot\omega(t)&=\frac{1}{J}\{T_u(t)-[T_\sigma(\theta)+T_s(\theta)+T_L(\theta)]+w_\omega(t)\}\\
\dot\sigma(t)&=\frac{E}{L}\{F_3(\theta)\omega(t)-[(1+S_f^i)v_R^i(t)-(1-S_b^{i+1})v_R^{i+1}+w_\xi(t)]\}\\
\dot T_u(t)&=-\frac{1}{\tau_{ATR}}T_u(t)+\frac{1}{\tau_{ATR}}T_u^{ref}(t)\\
\dot v_R^i(t)&=-\frac{1}{\tau_{ASR}}v_R^i+\frac{1}{\tau_{ASR}}v_R^{i,ref}(t)
\end{aligned} \tag{19}$$

where $F_3(\theta)=L_L[\sin(\theta+\beta)-\sin(\theta-\alpha)]$

$v_R^{i,ref}(t)$ and $T_u^{ref}(t)$ are the control inputs references of $v_R^i(t)$ and $T_u(t)$, respectively; τ_{ASR} and τ_{ATR} are the time constants of the first-order ASR and ATR systems, respectively. The control problem is to design control signals $v_R^{i,ref}(t)$ and $T_u^{ref}(t)$ so that $\theta(t)$ and $\sigma(t)$ track the reference values θ_r and σ_r respectively as exact as possible.

Since the fully nonlinear model given in Eqn. (19) is not suitable for controller design, the model is approximately linearized (by Taylor's series) about the output references θ_r and σ_r of the system, which could be expressed by

$$\begin{bmatrix}\Delta\dot\theta\\ \Delta\dot\omega\\ \Delta\dot\sigma\\ \Delta\dot T_u\\ \Delta\dot v_R^i\end{bmatrix}=\begin{bmatrix}0 & 1 & 0 & 0 & 0\\ -\frac{1}{J}\left(\frac{\partial T_{load}}{\partial\theta}\right) & 0 & -\frac{1}{J}\left(\frac{\partial T_\sigma}{\partial\sigma}\right) & \frac{1}{J} & 0\\ 0 & \frac{E}{L}F_3(\theta) & -\frac{E}{L}\left(\frac{\partial S_f^i}{\partial\sigma}v_R^i+\frac{\partial S_b^{i+1}}{\partial\sigma}v_R^{i+1}\right) & 0 & -\frac{E}{L}(1+S_f^i)\\ 0 & 0 & 0 & -\frac{1}{\tau_{ATR}} & 0\\ 0 & 0 & 0 & 0 & -\frac{1}{\tau_{ASR}}\end{bmatrix}\begin{bmatrix}\Delta\theta\\ \Delta\omega\\ \Delta\sigma\\ \Delta T_u\\ \Delta v_R^i\end{bmatrix}+$$

$$\begin{bmatrix} 0 & 0 \\ 0 & 0 \\ 0 & 0 \\ \dfrac{1}{\tau_{ATR}} & 0 \\ 0 & \dfrac{1}{\tau_{ASR}} \end{bmatrix} \begin{bmatrix} \Delta T_u^{ref}(t) \\ \Delta v_R^{i,ref}(t) \end{bmatrix} \tag{20}$$

The block diagram of the linearized model is given in Fig. 2.

In order to eliminate the steady state error, two state variables representing the integral of the output are introduced as follows:

$$\begin{cases} \Delta\dot{q}=\Delta\theta \\ \Delta\dot{p}=\Delta\sigma \end{cases} \tag{21}$$

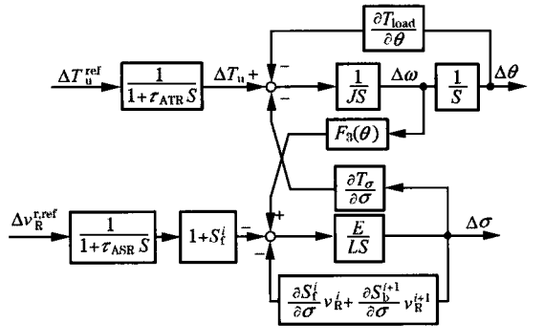

Fig. 2 Block diagram of linearized looper-tension system

1.4 Disturbances and unmodelled dynamics

There are disturbances and unmodelled dynamics from several sources which affect the looper and tension system.

For the tension loop, the main disturbance comes from the mass flow change. The change is mainly caused by the fast action of AGC systems in the case of temperature variations (skid marks) and thickness variations of the strip. Another disturbance is the set-up mismatch at the mills which creates a constant disturbance. Besides, the forward slip and backward slip, which are influenced by the time varying tension, are uncertain. Thus, an error of 5% in the nominal strip speed is frequently encountered. These disturbances and unmodelled dynamics are absorbed in the term:

$$w_\xi(t)=N+\delta(t) \tag{22}$$

where $N\in R$ is an unknown constant and $\delta(t)$ is totally unknown to the designer.

For the angle loop, disturbances and unmodelled dynamics come from the vicious friction phenomena of the hydraulic cylinder, the torque on the looper to bend the strip and so on. These disturbances and unmodelled dynamics are absorbed in $w_\omega(t)$. However, $w_\omega(t)$ is relatively small compared with $w_\xi(t)$. The speed perturbation $w_\xi(t)$ is the main source of disturbance.

2 Looper and Tension Control Structure

2.1 Conventional PID control schemes

There are mainly three kinds of conventional PID control schemes in the industry.

The first PI (proportional intergral) control algorithm, which is applied when tension is not available, only detects looper position. Tension is controlled by varying the torque supplied to the looper using LTCB (looper torque calculation block). And looper angle is controlled by the speed of the upstream main drive motor. The second PID control algorithm shown in Fig. 3, which will be used for comparison, adds tension feedback to the system. Tension is controlled by a PI regulator which acts on the input of ASR, and looper angle is controlled by a PID regulator which acts on the input of ATR. The last PID control algorithm works oppositely to the second one, that is, the control pairings is swapped: Tension is controlled by ATR, while looper angle is controlled by ASR.

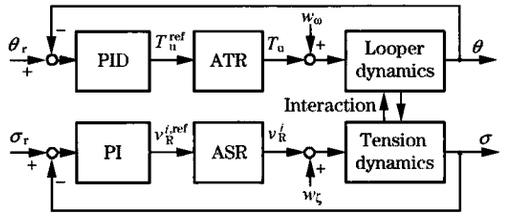

Fig. 3 Conventional PID control structure

Owing to their simplicity, the above conventional PID control techniques are common control methods in practice. However, these schemes result in slow responses and large deviations in both the tension and looper angle in the presence of disturbances and unmodelled dynamics. Due to the nonlinear nature of the system, the conventional PID control schemes have an obvious problem that high gain causes instability whereas low gain gives poor performances. Hence, to overcome the shortages of the conventional PID schemes, an alternative robust control scheme based on SMC is proposed.

2.2 Sliding mode control: a brief review

The SMC approach is regarded as one of the efficient tools to design robust controllers for both linear and nonlinear dynamic plants with uncertainties.

The major advantage of sliding mode is low sensitivity to system parameter variations and disturbances which eliminates the extremely difficult task of exact modelling. And SMC enables the decoupling of the overall system motion into independent partial components of lower dimension and as a result, reduces the complexity of feedback design. For the sake of completeness and the readers' conveniences, the problem of block control principle based on SMC is revisited for controllable linear systems $\dot{x}=Ax+Bu$ of the form:

$$\dot{x}_1=A_{11}x_1+A_{12}x_2 \tag{23}$$

$$\dot{x}_2=A_{21}x_1+A_{22}x_2+B_1u \tag{24}$$

where $x_1\in R^{n-m}$, $x_2\in R^m$, $u\in R^m$, $\det(B_1)\neq 0$ and $\mathrm{rank}(B_1)=\dim(u)$. Since the overall system is controllable, so does the pair (A_{11}, A_{12}). Assume Λ is the desired spectrum of the first subsystem Eqn. (23), as a result, the fictitious control of the first subsystem, x_2, can be given as

$$x_2=A_{12}^{+}(-A_{11}+\Lambda)x_1 \tag{25}$$

where A_{12}^{+} is the psudoinverse of A_{12}.

To implement the control design Eqn. (25), a sliding mode controller can be designed as

$$u=-B_1^{-1}M(x)\mathrm{sign}(s) \tag{26}$$

where

$$s=Cx=x_2-A_{12}^{+}(-A_{11}+\Lambda)x_1\in R^m,$$

$$C=\begin{bmatrix}c_1\\ \vdots\\ c_m\end{bmatrix}\in R^{m\times n} \text{ and } \mathrm{sign}(s)=\begin{bmatrix}\mathrm{sign}(s_1)\\ \vdots\\ \mathrm{sign}(s_m)\end{bmatrix} \tag{27}$$

And the diagonal matrix

$$M(x)=\begin{bmatrix}\alpha_1|x|+\delta_1 & & \\ & \ddots & \\ & & \alpha_m|x|+\delta_m\end{bmatrix} \tag{28}$$

where $|x|\in[|x_1|\cdots|x_n|]^{\mathrm{T}}$ and $\alpha_i\in R^{1\times n}$, $\delta_i\in R$, $i=1, \cdots, m$, are chosen so that the time derivative of the Lyapunov candidate function $V=(1/2)s^{\mathrm{T}}s$ is negative. To be specific, $\dot{V}$ can be calculated as

$$\dot{V}=s^{\mathrm{T}}\dot{s}=s^{\mathrm{T}}[C(Ax+Bu)]=s^{\mathrm{T}}[CAx]-$$

$$s^{\mathrm{T}}CBB_1^{-1}M(x)\mathrm{sign}(s)=[s_1\cdots s_m]\begin{bmatrix}c_1Ax\\ \vdots\\ c_mAx\end{bmatrix}-$$

$$[s_1\cdots s_m]\begin{bmatrix}\alpha_1|x|+\delta_1 & & \\ & \ddots & \\ & & \alpha_m|x|+\delta_m\end{bmatrix}\begin{bmatrix}\mathrm{sign}(s_1)\\ \vdots\\ \mathrm{sign}(s_m)\end{bmatrix}=$$

$$\sum_{i=1}^{m}[s_ic_iAx-|s_i|(\alpha_i|x|+\delta_i)] \tag{29}$$

where the forth step is from the fact that $CBB_1^{-1}=B_1B_1^{-1}=I_m$ [according to the definition of C in Eqn. (27)]. In order to set $\dot{V}$ negative, there are various approaches and the following approach is taken in this paper:

$$\alpha_i=|c_iA|\in R^{1\times n},\ \delta_i>0\in R,\ i=1,\cdots,m$$

It is evident that the negativity of $\dot{V}$ validates finite time convergence of the state vector to manifold $s=0$. When sliding mode is enforced, s is equal to zero, Eqn. (25) holds, and the system behaviour depends only on the first subsystem with desired dynamics

$$\dot{x}_1=\Lambda x_1 \tag{30}$$

And the time interval preceding the sliding motion may be decreased by increasing parameters δ_i in the controller. However, the discontinuous controller Eqn. (26) may lead to the well-known chattering effect due to the imperfection of the practical plants (small delays, dead zones, hysteresis and so on). The chattering drawback can be avoided by continuous approximation of the sign function as shown in Fig. 4. And the boundary ε is usually chosen according to the tradeoff between tracking performances and bandwidth limitations.

To summarize, the procedure for designing a sliding mode stabilizing controller usually contains the following three steps: designing the fictitious control Eqn. (25) to stabilize the reduced order subsystem Eqn. (23) with desired closed-loop dynamics Eqn. (30), taking the controller Eqn. (26) to validate finite time convergence of the state vector to the manifold $s=0$, and appropriate continuous approximation of the sign function, that is, the choosing of the boundary ε.

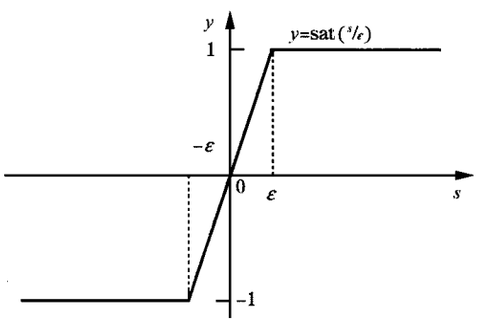

Fig. 4 Continuous approximation of sign function

2.3 Application of SMC to looper-tension control

To apply the SMC methodology, the looper-tension dynamics Eqn. (20) and Eqn. (21) need to be expressed in the form of Eqn. (23) and Eqn. (24). And for the sake of clarity and simplicity, the system model is calculated according to the values of the parameters given in Table 1 (obtained from the practical plant).

Table 1 Parameters of looper and tension system

Variable	Value	Unit	Variable	Value	Unit
θ_r	20	(°)	L_G	0.194	m
σ_r	8×10^6	Pa	R_r	0.0925	m
L_L	0.611	m	E	1.2×10^{10}	Pa
h_3	0.00908	m	d	1.5	m
h_4	0.00728	m	L	5.8	m
h_5	0.00547	m	L_1	2.34	m
R_w^i	0.4	m	L_2	3.46	m
R_w^{i+1}	0.4	m	ρ	7800	$kg\cdot m^{-3}$
v_R^i	6.058	m/s	τ_{ASR}	0.04	s^{-1}
v_R^{i+1}	8.596	m/s	τ_{ATR}	0.01	s^{-1}
S_f^i	0.05		g	9.8	m/s^2
S_b^{i+1}	0.2		L_3	0.195	m
M_L	1862.9	kg	J	172.65	$kg\cdot m^2$

Thus,

$$\begin{bmatrix}\Delta\dot q\\ \Delta\dot\theta\\ \Delta\dot\omega\\ \Delta\dot p\\ \Delta\dot\sigma\end{bmatrix}=\begin{bmatrix}0&1&0&0&0\\0&0&1&0&0\\0&-97.3&0&0&-153\\0&0&0&0&1\\0&0&1.52&0&-3.27\end{bmatrix}\begin{bmatrix}\Delta q\\ \Delta\theta\\ \Delta\omega\\ \Delta p\\ \Delta\sigma\end{bmatrix}+\begin{bmatrix}0&0\\0&0\\332&0\\0&0\\0&-21.7\end{bmatrix}\begin{bmatrix}\Delta T_u\\ \Delta v_R^i\end{bmatrix}\tag{31}$$

$$\begin{bmatrix}\Delta\dot T_u\\ \Delta\dot v_R^i\end{bmatrix}=\begin{bmatrix}-100&0\\0&-25\end{bmatrix}\begin{bmatrix}\Delta T_u\\ \Delta v_R^i\end{bmatrix}+\begin{bmatrix}100&0\\0&25\end{bmatrix}\begin{bmatrix}\Delta T_u^{ref}(t)\\ \Delta v_R^{i,\,ref}(t)\end{bmatrix}\tag{32}$$

Concerning the first subsystem Eqn. (31), ΔT_u and Δv_R^i are fictitious control inputs. For the angle loop, with $[\Delta q\ \Delta\theta\ \Delta\omega]^T$ as states, the state equation is of canonical form except for an interaction with $\Delta\sigma$ in $\Delta\dot\omega$. This undesirable interaction can easily be cancelled by including an opposite item in the fictitious control input ΔT_u. And the same spirit can be applied to the tension loop. As a result, it is easy to design state feedback control law achieving system decoupling and pole assignment for the first subsystem. According to the target time constants of the control system, $\lambda_1^q=-2$, $\lambda_2^q=-6$, $\lambda_3^q=-20$, and $\lambda_1^\sigma=-3$, $\lambda_2^\sigma=-9$ are chosen as desired poles for the angle loop and the tension loop respectively. Thus, the fictitious state feedback control law will be designed as

$$\begin{bmatrix}\Delta T_u\\ \Delta v_R^i\end{bmatrix}=-\begin{bmatrix}0.72&0.225&0.084&0&-0.46\\0&0&-0.07&-1.24&-0.40\end{bmatrix}\begin{bmatrix}\Delta q\\ \Delta\theta\\ \Delta\omega\\ \Delta p\\ \Delta\sigma\end{bmatrix}\tag{33}$$

And the closed-loop system will be of the form

$$\begin{bmatrix}\Delta\dot q\\ \Delta\dot\theta\\ \Delta\dot\omega\\ \Delta\dot p\\ \Delta\dot\sigma\end{bmatrix}=\begin{bmatrix}0&1&0&0&0\\0&0&1&0&0\\-240&-172&-28&0&0\\0&0&0&0&1\\0&0&0&-27&-12\end{bmatrix}\begin{bmatrix}\Delta q\\ \Delta\theta\\ \Delta\omega\\ \Delta p\\ \Delta\sigma\end{bmatrix}\tag{34}$$

which is completely decoupled and of desired dynamics.

As can be seen from the SMC design procedure discussed in Section 2.2, once the fictitious control inputs Eqn. (33) are given, the sliding manifold should be chosen as

$$s=\begin{bmatrix}s_1\\ s_2\end{bmatrix}=\begin{bmatrix}c_1\\ c_2\end{bmatrix}x=\begin{bmatrix}0.72&0.225&0.084&0&-0.46&1&0\\0&0&-0.07&-1.24&-0.40&0&1\end{bmatrix}\begin{bmatrix}\Delta q\\ \Delta\theta\\ \Delta\omega\\ \Delta p\\ \Delta\sigma\\ \Delta T_u\\ \Delta v_R^i\end{bmatrix}\tag{35}$$

Consequently, the sliding mode controller is designed as

$$u=-B_1^{-1}\begin{bmatrix}\alpha_1|x|+\delta_1&\\&\alpha_2|x|+\delta_2\end{bmatrix}\begin{bmatrix}\mathrm{sat}(s_1/\varepsilon_1)\\ \mathrm{sat}(s_2/\varepsilon_2)\end{bmatrix}\tag{36}$$

where saturation function sat() is shown in Fig. 4 and $B_1=\begin{bmatrix}100&0\\0&25\end{bmatrix}$,

$\alpha_1=|c_1A|=[0\ 7.5\ 0.48\ 0\ 11.4\ 72\ 10]$,

$\alpha_2=|c_2A|=[0\ 6.8\ 0.6\ 0\ 10.8\ 23\ 16]$, $\delta_1=25$, $\delta_2=20$ *and* $\varepsilon_1=0.5$, $\varepsilon_2=0.4$.

And the overall control structure is given in Fig. 5.

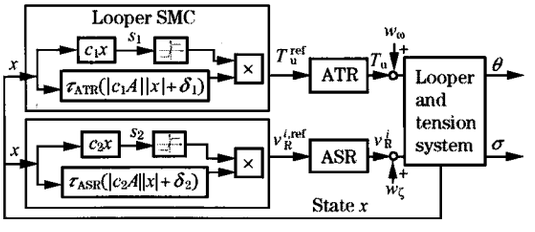

Fig. 5 Sliding mode control structure

3 Simulation Results

Dynamic simulations using Matlab are carried out to evaluate the performances of the proposed SMC controllers. The simulations are performed on a fully nonlinear model tuned in agreement with the practical plant and adequately grasp the dynamic behavior of the finishing mill. Therefore, they are very useful for tasks such as high performance control design and evaluation. For the sake of comparison, simulation results of the conventional PID algorithm given in Fig. 3 are also reported. And the PID regulators are developed by on-line tuning over many years.

The results reported are for Looper 4 in a seven-stand finishing mill. The looper angle reference θ_r is 20° and the strip tension reference σ_r is 8 MPa. Simulation results are plotted from Fig. 6 to Fig. 8, where solid lines are the results for SMC controllers and dashed lines for PID controllers. Several characteristic disturbances are included in the simulation analysis. The outputs and inputs of the system in the presence of strip speed step disturbance $w_\xi = -1$ cm/s and looper torque step disturbance $w_\omega = 0.5$ kN • m are shown in Fig. 6 and Fig. 7, respectively. Fig. 8 presents the responses of the system in the case of the persisting disturbances

$w_\xi(t) = -1 - 0.4[\sin(10t+3) + \sin(7t)]$ cm/s

and $w_\omega(t) = 0.5\sin(20t)$ kN • m

which are designed according to Section 1.4 and the characteristics of the real plant. In general terms, the disturbances are more critical than the real case.

As indicated by the simulation results, the conventional PID controllers result in long settling time, and the deviations in both the tension and looper angle are greater than desired values in the presence of disturbances and unmodelled dynamics. Besides, the interaction between the tension loop and the angle loop is serious: w_ξ and w_ω bring obvious

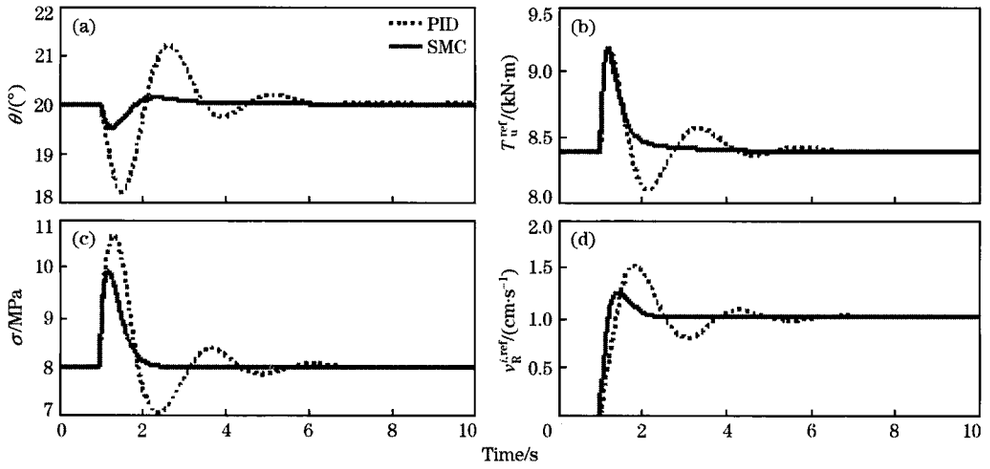

Fig. 6 Outputs and inputs of system in presence of strip speed step disturbance $w_\xi(t) = -1$ cm/s active for $t > 1$ s

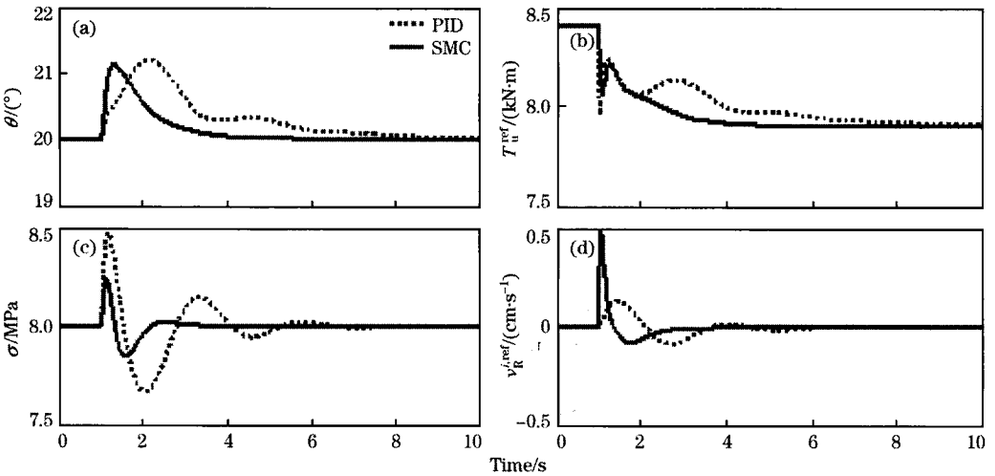

Fig. 7 Outputs and inputs of system in presence of looper torque step disturbance $w_\omega(t) = 0.5$ kN • m active for $t > 1$ s

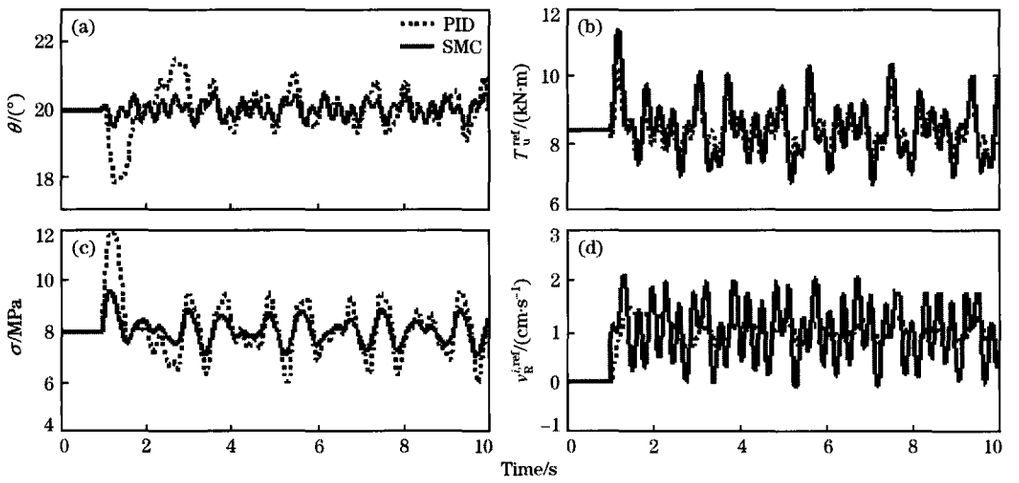

Fig. 8 Outputs and inputs of system in presence of looper torque disturbance $w_\omega(t)=0.5\sin(20t)$ kN · m and strip speed disturbance $w_\xi(t)=-1-0.4[\sin(10t+3)+\sin(7t)]$ cm/s active for $t>1$ s

deviations in both the tension and angle. In the case of the controllers proposed in this paper, the settling time and deviations due to the persisting disturbances are greatly reduced with respect to PID controllers (Fig. 8). Furthermore, owing to the decoupling design of the reduced order subsystem, the tension loop and the angle loop are generally decoupled. w_ξ only brings obvious deviation in the tension (Fig. 6), while deviation in the tension caused by w_ω is smaller than usual (Fig. 7). However, the SMC controllers achieve better dynamic performances with higher control efforts (the control input of ASR in Fig. 8 especially).

4 Conclusions

An innovative looper and tension sliding mode control approach based on approximately linearized model is investigated in this paper. The input-output relations of the looper and tension dynamics are decoupled on the sliding manifold. Thus, the interaction between the looper angle and tension is less serious than usual. Simulation results show the effectiveness of the proposed method which is robust to unmodelled dynamics, simple in structure and more adequate for application.

However, since the stand and interstand are tightly coupled, future research efforts will be devoted to take the interactions between the strip tension, strip thickness (gauge) and looper angle into account. Another research trend could be the extending of the proposed approach to the integral control problem consisting of seven stands and six loopers.

References:

[1] SUN Jie, ZHANG Dian-hua, LI Xu, et al. Smith Prediction Monitor AGC System Based on Fuzzy Self-Tuning PID Control [J]. Journal of Iron and Steel Research, International, 2010, 17(2): 22.

[2] DU Xiao-zhong, YANG Quan, LU Cheng, et al. Optimization of Short Stroke Control Preset for Automatic Width Control of Hot Rolling Mill [J]. Journal of Iron and Steel Research, International, 2010, 17(6): 16.

[3] LI Hai-jun, XU Jian-zhong, WANG Guo-dong, et al. Development of Strip Flatness and Crown Control Model for Hot Strip Mills [J]. Journal of Iron and Steel Research, International, 2010, 17(3): 21.

[4] ZHENG Shen-bai, HAN Jing-tao, WANG Jiang. Kinematic Mechanics Steady Equation of Continuous Rolling Tension [J]. Journal of Iron and Steel Research, 2005, 17(6): 39 (in Chinese).

[5] LI Bo-qun, ZHANG Ke-jun, FU Jian, et al. Adaptive Neural Network Decoupling Control for the Loopers' Height and Tension System [J]. Control and Decision, 2006, 21(1): 46 (in Chinese).

[6] LIU Tong-feng, MU Zhi-chun. Looper Decoupling Control for Hot Strip Mill Based on Differential Geometry [J]. Control Engineering of China, 2007, 14(6): 580 (in Chinese).

[7] LI Xu, ZHANG Dian-hua, ZHOU Na, et al. Decoupling Looper Height and Tension Control System With Characteristic Locus Method [J]. Information and Control, 2005, 34(6): 665 (in Chinese).

[8] FU Xing-jian, TONG Chao-nan, ZONG Sheng-yue. H-∞ Control and Simulation Study for Looper System of Hot Strip Rolling Mill [J]. Journal of System Simulation, 2006, 18(1): 162 (in Chinese).

[9] Furlan R, Cuzzola F A, Parisini T. Friction Compensation in the Interstand Looper of Hot Strip Mills: A Sliding-Mode Control Approach [J]. Control Engineering Practice, 2008, 16(2): 214.

[10] TONG Chao-nan, WU Yan-kun, LIU Lei-ming, et al. Modeling and Integral Variable Structure Control of Hydraulic Looper Multivariable System [J]. Acta Automatica Sinica, 2008, 34(10): 1305 (in Chinese).